Original Research

Implication of Bcl-2-associated athanogene 3 in fibroblast growth factor-2-mediated epithelial–mesenchymal transition in renal epithelial cells

Feng Du[1], Si Li[2], Tian Wang[2], Hai-Yan Zhang[3], De-Tian Li[1], Zhen-Xian Du[2] and Hua-Qin Wang[4]

[1]Department of Nephrology, Shengjing Hospital, China Medical University, Shenyang 110004, China; [2]Department of Endocrinology and Metabolism, the 1st Affiliated Hospital, China Medical University, Shenyang 110001, China; [3]Department of Geriatrics, the 1st Affiliated Hospital, China Medical University, Shenyang 110001, China; [4]Department of Biochemistry and Molecular Biology, China Medical University, Shenyang 110001, China

Corresponding author: Feng Du. Email: dolphine_doctor@hotmail.com

Abstract

The epithelial–mesenchymal transition (EMT) of tubular epithelial cells to myofibroblast-like cells plays a substantial role in renal tubulointerstitial fibrosis, which is a common pathological character of end-stage renal disease (ESRD). Fibroblast growth factor-2 (FGF-2) triggers EMT in tubular epithelial cells and increases Bcl-2-associated athanogene 3 (BAG3) expression in neural progenitor and neuroblastoma cells. In addition, a novel role of regulation of EMT has been ascribed to BAG3 recently. These previous reports urged us to study the potential involvement of BAG3 in EMT triggered by FGF-2 in renal tubular epithelial cells. The current study found that FGF-2 induced EMT, simultaneously increased BAG3 expression in human kidney 2 (HK2) cells. Although FGF-2 induced EMT in nontransfected or scramble short hairpin RNA (shRNA) transfected HK2 cells, it was ineffective in BAG3-silenced cells, indicating a favorable role of BAG3 in EMT of tubular cells induced by FGF-2. Knockdown of BAG3 also significantly suppressed motion and invasion of HK2 cells mediated by FGF-2. Furthermore, we confirmed that BAG3 was upregulated in kidney of unilateral ureteral obstruction (UUO) rats, a well-established renal fibrosis model, in which EMT is supposed to exert a substantial influence on renal fibrosis. Importantly, upregulation of BAG3 was limited to tubular epithelial cells. Results of the current study identify BAG3 as a potential player in EMT of tubular epithelial cells, as well as renal fibrosis.

Keywords: BAG3, EMT, FGF-2, tubular epithelial cell

***Experimental Biology and Medicine* 2015; 240: 566–575. DOI: 10.1177/1535370214558023**

Introduction

Renal tubulointerstitial fibrosis is characterized by extracellular matrix deposition and the extent of fibrosis is an excellent prognostic marker for end-stage renal disease (ESRD).[1,2] Epithelial–mesenchymal transition (EMT) of renal tubular epithelial cells into myofibroblasts has been reported to play a substantial role in renal fibrosis.[2–8] EMT is a well-orchestrated transcriptional and morphological process, during which epithelial cells lose their epithelial features and coincide with the acquisition of a mesenchymal phenotype.[9–11] During EMT procedure, epithelial markers, e.g. E-cadherin and the zonula occludens protein-1 (ZO-1) are reduced, while mesenchymal markers, such as α-smooth muscle actin (α-SMA), fibronectin, vimentin (VIM) are increased.[7] Along with morphological changes, cells undergoing EMT acquire migratory and invasive abilities, which allow escape from the epithelium into peripheral tissues.[9–11]

Various factors, such as profibrotic cytokines, growth factors, advanced glycation end products, hypoxia, and reactive oxygen species, have been reported to induce EMT in renal tubular epithelial cells.[6] Fibroblast growth factor-2 (FGF-2) has been demonstrated to play a substantial role in proliferation and differentiation of various cell types. FGF-2 also plays an important role in the induction of EMT in renal tubular epithelial cells.[12,13] It has been reported that FGF-2 increases the expression of mesenchymal markers VIM and α-SMA, promotes the release of matrix metallopeptidase-9 (MMP-9) and MMP-2, and also reduces the expression of epithelial markers cytokeratin and E-cadherin in renal tubular epithelial cells.[12,13]

Bcl-2-associated athanogene 3 (BAG3) has been initially identified as an interacting partner of Bcl-2 using yeast two hybridization.[14] Expression of BAG3 is limited to the striated muscle cells, including the skeletal muscle cells and the myocardiac cells,[15–17] but its expression is induced by many stress

stimuli, such as high temperature, heavy metal exposure, and some chemotherapeutic drugs.[18–23] BAG3 is involved in various biological functions, such as cell survival, cell cycle progression, apoptosis, autophagy, regulation of viral infection, cell adhesion, and invasion.[24–30] Recently, we have identified a novel role of BAG3 in regulation of EMT in thyroid cancer cells.[31] Coupled with the fact that BAG3 expression is increased in neuron progenitor and neuroblastoma cells treated with FGF-2,[32,33] these previous reports urged us to determine whether BAG3 is potentially involved in EMT of renal epithelial cells mediated by FGF-2. In this paper, we report that BAG3 was increased upon EMT mediated by FGF-2 in human kidney 2 (HK2) cells. In addition, the current study demonstrates that suppression of BAG3 inhibits EMT, motion, and invasion of HK2 cells induced by FGF-2. Importantly, we also provide *in vivo* data indicative of the involvement of BAG3 in renal fibrosis. Collectively, these findings set BAG3 as a potential target to prevent and/or treat renal fibrosis.

Result

Induction of BAG3 expression by FGF-2 in HK2 cells

HK2 cells were treated with various concentrations of FGF-2 for 24 h, and the expression of BAG3 and mesenchymal markers was evaluated by quantitative real-time polymerase chain reaction (PCR). Treatment with FGF-2 triggered a significant increase in BAG3 mRNA expression in a dose-dependent pattern (Figure 1(a)). Consistent with the role of FGF-2 in EMT induction in the proximal tubular epithelium, FGF-2 significantly increased α-SMA and VIM expression at the mRNA level in HK2 cells (Figure 1(b)). The induction of BAG3, α-SMA, and VIM protein synthesis was also confirmed by Western blot analysis (Figure 1(c)). Since FGF-2 activates several signaling pathways including extracellular signal-regulated kinase (ERK), phosphatidylinositol-3-kinase (PI3K)/Akt, and protein kinase C (PKCδ), their relative specific inhibitors were used to investigate their possible involvement in upregulation of BAG3 mediated by FGF-2. Real-time PCR showed that 10 μM of LY294002, the PI3K/Akt inhibitor, significantly blocked induction of BAG3 mediated by FGF-2, while neither 5 μM of U0126 (specific ERK inhibitor) nor 5 μM of rottlerin (specific PKCδ inhibitor) demonstrated obvious effects on BAG3 increase induced by FGF-2 (Figure 1(d)). Western blot confirmed that LY294002 significantly decreased BAG3 expression, while no obvious alteration was observed in cells treated with U0126 or rottlerin (Figure 1(e)).

The role of BAG3 on expression of mesenchymal markers

To investigate the functional implication of BAG3 in EMT of HK2 cells, lentiviral plasmids containing sequences specific

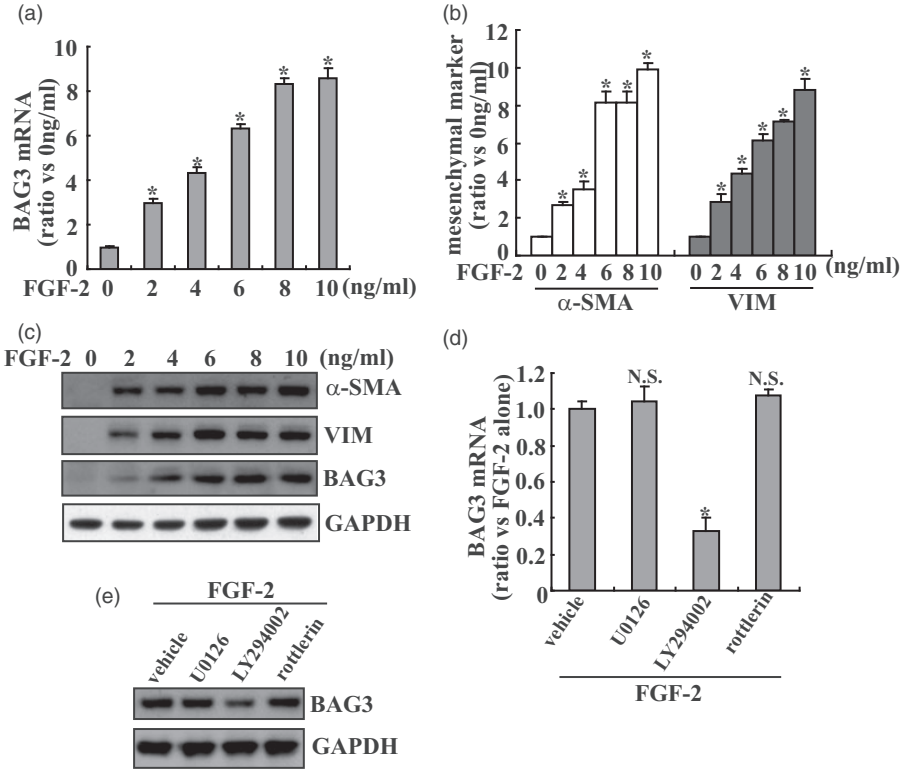

Figure 1 Increase in BAG3 expression in HK2 cells exposed to FGF-2. (a) HK2 cells were treated with the indicated dose of FGF-2 for 24 h, BAG3 mRNA was measured using real-time RT-PCR. (b) HK2 cells were treated with the indicated dose of FGF-2 for 24 h, mRNA levels of mesenchymal markers α-SMA and VIM were analyzed using real-time RT-PCR. (c) HK2 cells were treated with the indicated dose of FGF-2 for 24 h, Western blot analysis was performed using the indicated antibodies. (d) HK2 cells were pretreated with vehicle, 5 μM of U0126, 10 μM of LY294002, or 5 μM of rottlerin for 30 min, then treated with 10 ng/mL of FGF-2 for additional 24 h, real-time RT-PCR was performed to investigate BAG3 mRNA expression. (e) HK2 cells were pretreated with vehicle, 5 μM of U0126, 10 μM of LY294002, or 5 μM of rottlerin for 30 min, then treated with 10 ng/mL of FGF-2 for additional 24 h, BAG3 protein expression was measured using Western blot analysis. *$P < .01$. N.S.: not significant; BAG3: Bcl-2-associated athanogene 3; FGF-2: fibroblast growth factor-2

against BAG3 (siBAG3) were used to knockdown the BAG3 expression. Measurement of green fluorescent protein (GFP) positive cells by fluorescence microscopy demonstrated that transduction efficiency by lentiviral vectors was >90% (Figure 2(a)). Real-time PCR (Figure 2(b)) and Western blot (Figure 2(c)) confirmed that two different siBAG3 types (#2 and #4) significantly decreased BAG3 expression in HK2 cells treated with 10 ng/mL of FGF-2, while scrambled

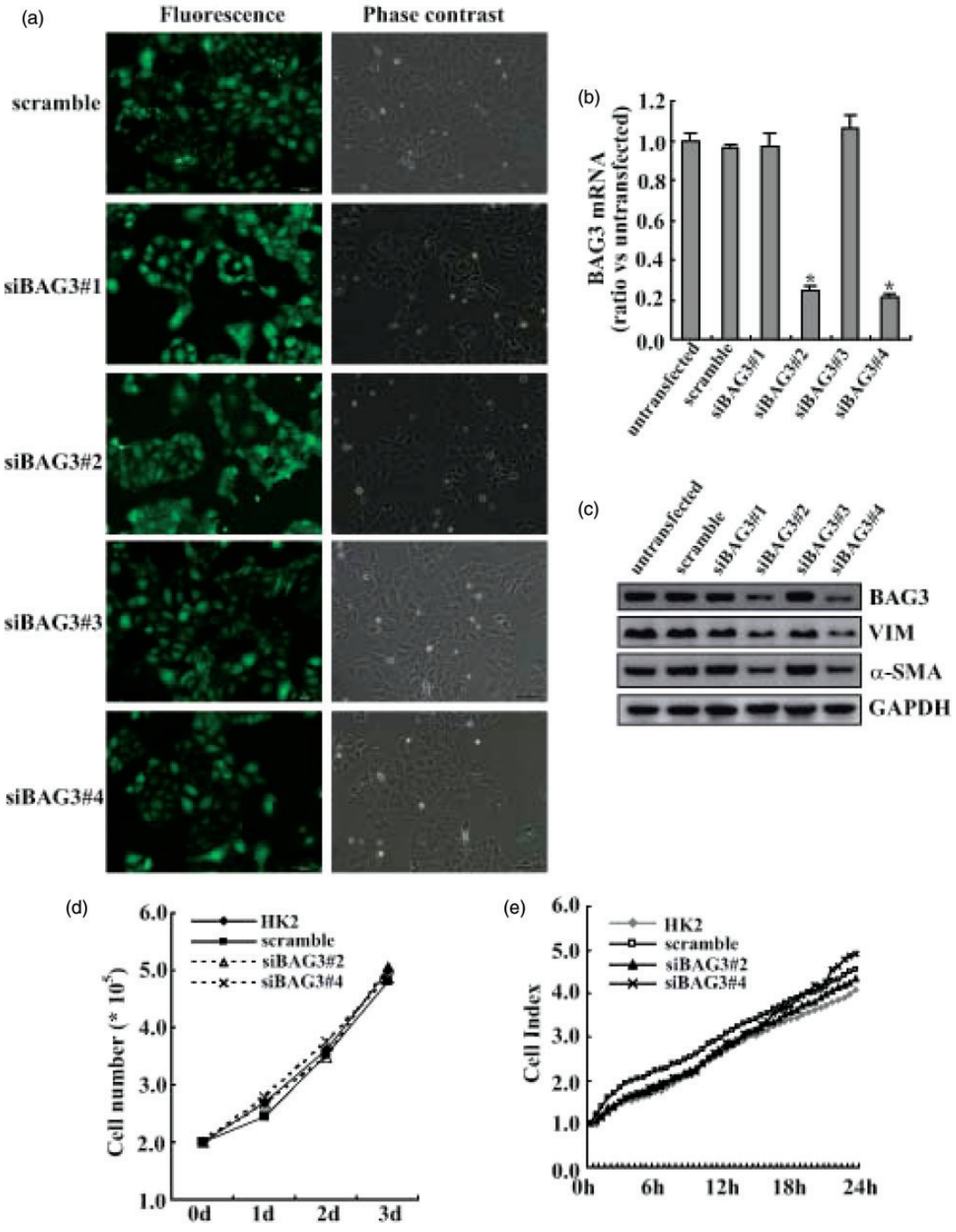

Figure 2 Attenuation of FGF-2-mediated increases in mesenchymal makers by BAG3 knockdown. (a) HK2 cells were transduced with 100 multiplicity of infection (MOI) of lentiviral vectors containing BAG3 siRNA (siBAG3) or control (CON) siRNA (scramble) target sequences for 12 h, then cultured for additional 48 h, and GFP positive cells were observed under a fluorescence microscopy. (b) HK2 cells were transduced with siBAG3 or scramble lentiviral vectors for 12 h and cultured for additional 48 h. Cells were then treated with 10 ng/mL of FGF-2 for additional 24 h and BAG3 mRNA was analyzed using real-time RT-PCR. (c) HK2 cells were transduced with siBAG3 or scramble lentiviral vectors for 12 h and cultured for additional 48 h. Cells were then treated with 10 ng/mL of FGF-2 for additional 24 h and Western blot was performed using the indicated antibodies. (d) HK2 cells were transduced with siBAG3 or scramble lentiviral vectors for 12 h and cultured for additional 48 h. Viable cells were then counted using trypan blue exclusion experiment. (e) HK2 cells were transduced with siBAG3 or scramble lentiviral vectors for 12 h and cultured for additional 48 h. Cell proliferation was measured using RTCA system in a real-time setting within 24 h of culture. N.S.: not significant; BAG3: Bcl-2-associated athanogene 3; VIM: vimentin; α-SMA: α-smooth muscle actin; HK2: human kidney 2. *$P < .01$. (A color version of this figure is available in the online journal.)

siRNA, siBAG3#1, or siBAG3#3 demonstrated no obvious effects (Figure 2(c)). Importantly, knockdown of BAG3 by siBAG3#2 and siBAG3#4 significantly decreased VIM and α-SMA expression upon exposure to FGF-2 (Figure 2(c)). Trypan blue experiments demonstrated that BAG3 knockdown had little influence on cell proliferation under basal culture conditions (Figure 2(d)). We also measured cell proliferation using real-time cell analyzer (RTCA) and confirmed that knockdown of BAG3 demonstrated no obvious influence on proliferation of HK2 cells (Figure 2(e)).

Effects of BAG3 on morphological changes induced by FGF-2 in HK2 cells

When grown in serum-free conditions, parent and scrambled siRNA-infected HK2 cells appeared as a typical 'cobblestone' monolayer. No obvious morphological changes were observed in either siBAG3#2 or siBAG3#4-infected cells under basal conditions (Figure 3(a)). After five days of FGF-2 exposure, parent and scrambled siRNA-infected HK2 cells became elongated and acquired a spindle-shaped morphology (Figure 3(a)). However, siBAG3#2 and siBAG3#4-infected HK2 cells only exhibited a little scattered distribution, but no obvious morphological alterations were observed at this time point (Figure 3(a)). We also investigated cytoskeleton organization by staining cells with phalloidin, and confirmed that knockdown of BAG3 significantly blocked the morphological change of HK2 cells mediated by FGF-2 treatment (Figure 3(b)). Quantitative morphometric analysis showed that the ratio of major axis *versus* minor axis was significantly increased in uninfected and scrambled siRNA-infected HK2 cells treated with FGF-2, while the increase was apparently suppressed in siBAG3#2 and siBAG3#4 lentivirus-infected cells (Figure 3(c)).

Regulation of FGF-2-mediated motion and invasion of HK2 cells by BAG3

To investigate the influence of BAG3 on motive and invasive capacity of HK2 cells upon FGF-2 exposure, wound healing, and Transwell assays were performed. The wound-healing assay demonstrated that knockdown of BAG3 by siBAG3#2 or siBAG3#4 had no obvious effect on the motion of HK2 under normal culture conditions (Figure 4(a)). However, motion of HK2 cells was significantly suppressed in siBAG3#2 and siBAG3#4-infected cells, while scrambled siRNA demonstrated no obvious influence when compared with parent HK2 cells upon treatment with FGF-2 (Figure 4(b)). Invasive capacity of HK2 cells induced by FGF-2 was measured using a Transwell system with matrigel-coated membrane, which demonstrated that the numbers of cells passed through the membrane were significantly decreased in BAG3 knockdown cells (Figure 4(c,d)).

Distribution of BAG3 in kidneys from unilateral ureteral obstruction (UUO) rats

To study the potential involvement of BAG3 in renal tubular EMT *in vivo*, we used UUO rats, a well-established renal fibrosis animal model, with EMT being an important player.[34,35] To address cellular localization of BAG3, immunohistochemical staining of BAG3 was performed using kidney sections from rats with sham and UUO operation. Hematoxylin and eosin (HE) staining demonstrated that the renal structures were severely damaged at 14 days after UUO operation (Figure 5(a)). Masson staining confirmed that UUO operation resulted in an accumulation of collagen in the kidneys (Figure 5(b)). α-SMA immunohistochemical staining demonstrated that its immunoreactivity was significantly increased in tubular epithelial cells from UUO-operated kidneys, confirming the occurrence of renal EMT after UUO operation (Figure 5(c)). Immunohistochemical analysis showed that no or little expression of BAG3 protein was observed throughout the sections from sham-operated control rats, while positive BAG3 staining appeared in renal tubular epithelial cells at day 14 after the UUO operation (Figure 5(d)).

Discussion

Consistent with previous reports,[12,13] the current study confirmed that FGF-2 induced a significant increase in α-SMA and VIM expression in HK2 cells, reflecting a transition toward the mesenchymal phenotype. BAG3 is one of the BAG co-chaperone family members, which was first screened as a binding protein with Bcl-2.[15,36,37] Multiple functions have been assigned to BAG3, and recently its involvement in EMT of thyroid cancer cells has been reported.[31] However, the function of BAG3 in renal fibrosis is still unknown. The current study demonstrated that BAG3 was significantly increased upon exposure of HK2 cells to FGF-2. Using specific kinase inhibitors, the current study demonstrated that PI3K/Akt signal was implicated in upregulation of BAG3 mediated by FGF-2, but not ERK or PKCδ signal. In our cellular model of BAG3-silenced cells, the basal expression α-SMA and VIM was much the same as in noninfected or scramble short hairpin RNA (shRNA)-infected HK2 cells. However, the increase in response to FGF-2 stimulation was markedly suppressed in BAG3-silenced cells. We also found that knockdown of BAG3 suppressed morphological alterations, motion, and invasion of HK2 cells mediated by FGF-2, supporting a favorable function of BAG3 in EMT and invasion of renal tubular cells.

UUO is a well-known animal model with progressive interstitial fibrosis,[38] in which EMT has been reported to play a critical role.[39] Using immunohistochemical staining, the current study reported that BAG3 was specifically upregulated in the tubular epithelium of kidneys from UUO rats. Coupled with the data from cells exposed to FGF-2, the current study suggests that BAG3 might be generally involved in renal EMT. Further investigation on its influences on other stimulators, such as transforming growth factor (TGF) β-induced EMT of tubular epithelial cells, might enhance our understanding of its role in renal fibrosis. Furthermore, a study of the impact of BAG3 suppression in the UUO model in the future might clarify its potential involvement in renal fibrosis *in vivo*, which might set BAG3 as a potential target for prevention and/or treatment of renal fibrosis.

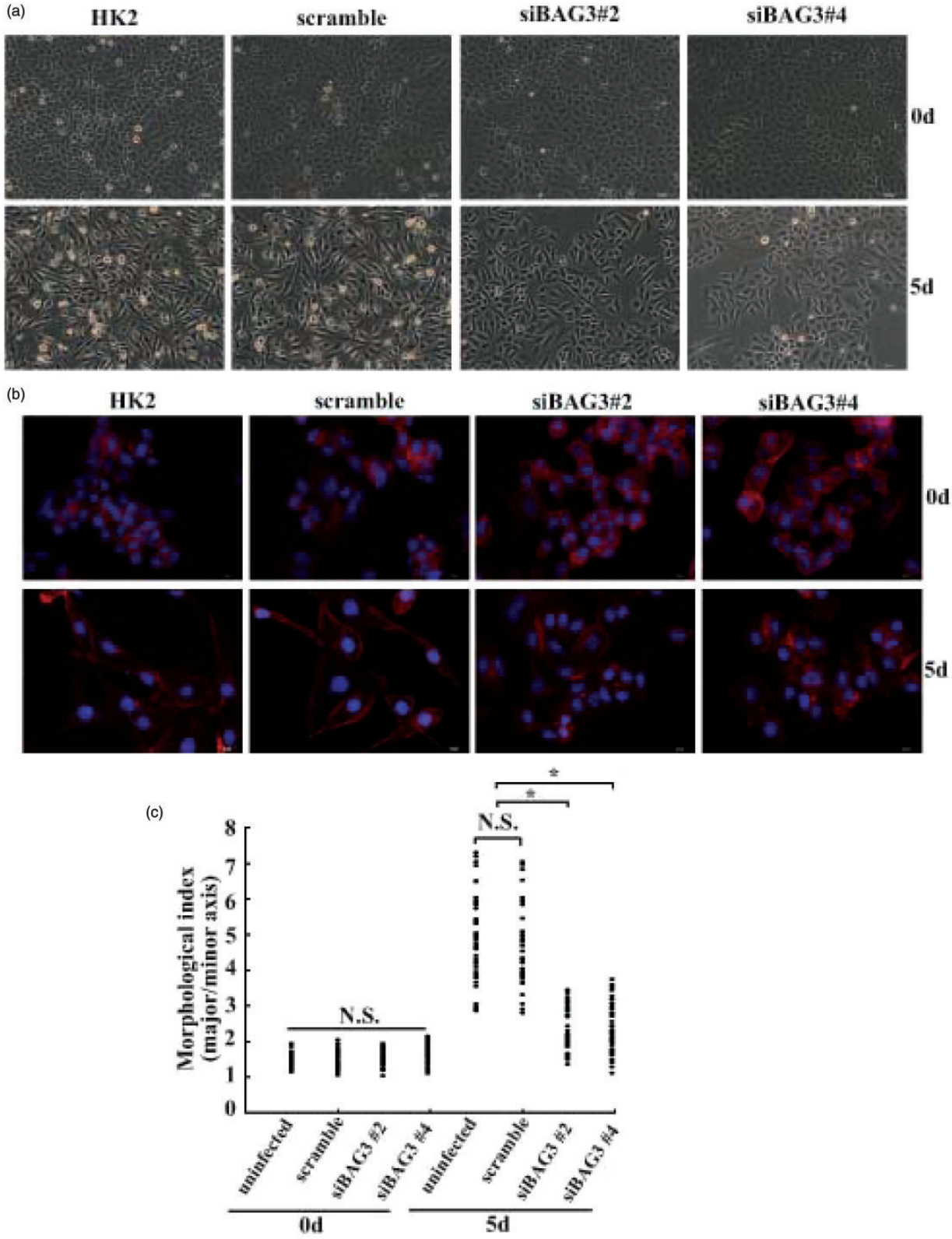

Figure 3 Suppression of FGF-2-mediated morphological alterations of HK2 cells by BAG3 knockdown. (a) HK2 cells were transduced with siBAG3 or scramble lentiviral vectors for 12 h and cultured for additional 48 h. Cells were then treated with 10 ng/mL of FGF-2 for five days and cell morphology was observed under a phase contrast microscopy. (b) HK2 cells were transduced with siBAG3 or scramble lentiviral vectors for 12 h and cultured for additional 48 h. Cells were then treated with 10 ng/mL of FGF-2 for five days and stained with phalloidin (red) and nucleus with DAPI (blue). (c) Quantitative analysis of the degree of elongated cell morphology or morphological index in (b). Representative data shown are from a single experiment, for which *n* was at least 50 for each cell type. Similar data was obtained from three independent cell preparations. N.S.: not significant; HK2: human kidney 2. $^*P < .01$. (A color version of this figure is available in the online journal.)

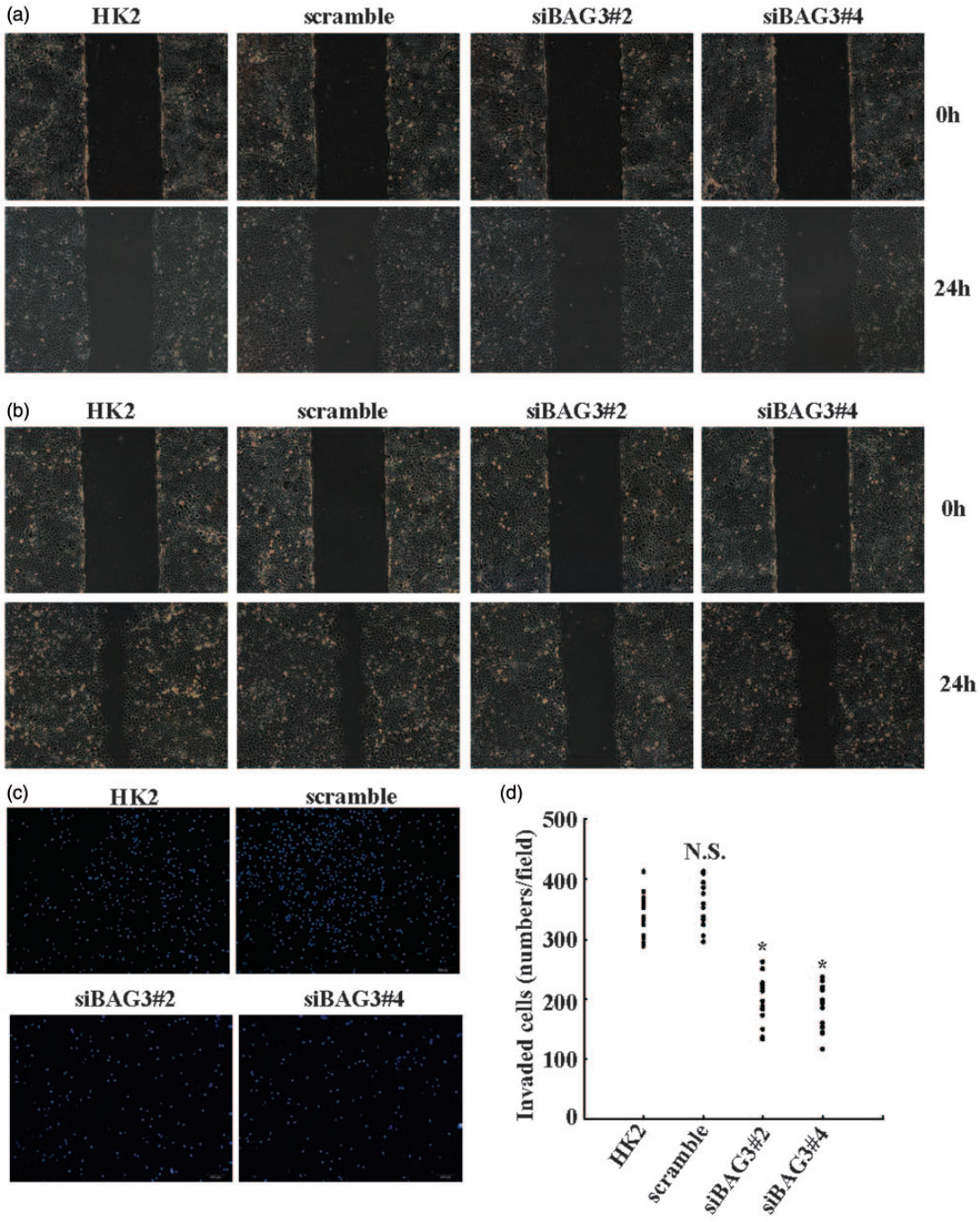

Figure 4 Suppression of FGF-2-mediated motion and invasion of HK2 cells by BAG3 knockdown. (a) HK2 cells were transduced with siBAG3 or scramble lentiviral vectors for 12 h and cultured for additional 48 h. Cell motility was analyzed using wound-healing assays. (b) HK2 cells were transduced with siBAG3 or scramble lentiviral vectors for 12 h and cultured for additional 48 h. Cells were then treated with 10 ng/mL of FGF-2 and cell motion was evaluated using wound-healing assays. (c) HK2 cells were transduced with siBAG3 or scramble lentiviral vectors for 12 h and cultured for additional 48 h. Cells were then treated with 10 ng/mL of FGF-2 and cell invasion was evaluated by Matrigel-coated Transwell system. (d) Cells that have passed through Matrigel-coated membrane in (c) were counted in five representative microscopic fields and three independent experiments were performed. Cell numbers for each count were plotted in the graph. N.S.: not significant; HK2: human kidney 2. *$P < .01$. (A color version of this figure is available in the online journal.)

We have recently reported a novel role of BAG3 in the EMT of thyroid cancer cells.[31] PKCδ-mediated phosphorylation at Ser187 site appears to play a critical role, as phosphorylated and unphosphorylated forms of BAG3 demonstrate completely opposite effects on EMT of thyroid cancer cells.[31] Due to the lack of a specific antibody to identify phosphorylated BAG3, the current study could not determine which form of BAG3 was implicated in the EMT of HK2 cells mediated by FGF-2. As numerous functions of FGF-2 have been ascribed to PKCδ activation,[40–43] we thus speculated that, similarly with thyroid cancer cells, a phosphorylated form of BAG3 might be responsible for the EMT of HK2 induced by FGF-2. The generation of an antibody to specifically recognize phosphorylated BAG3

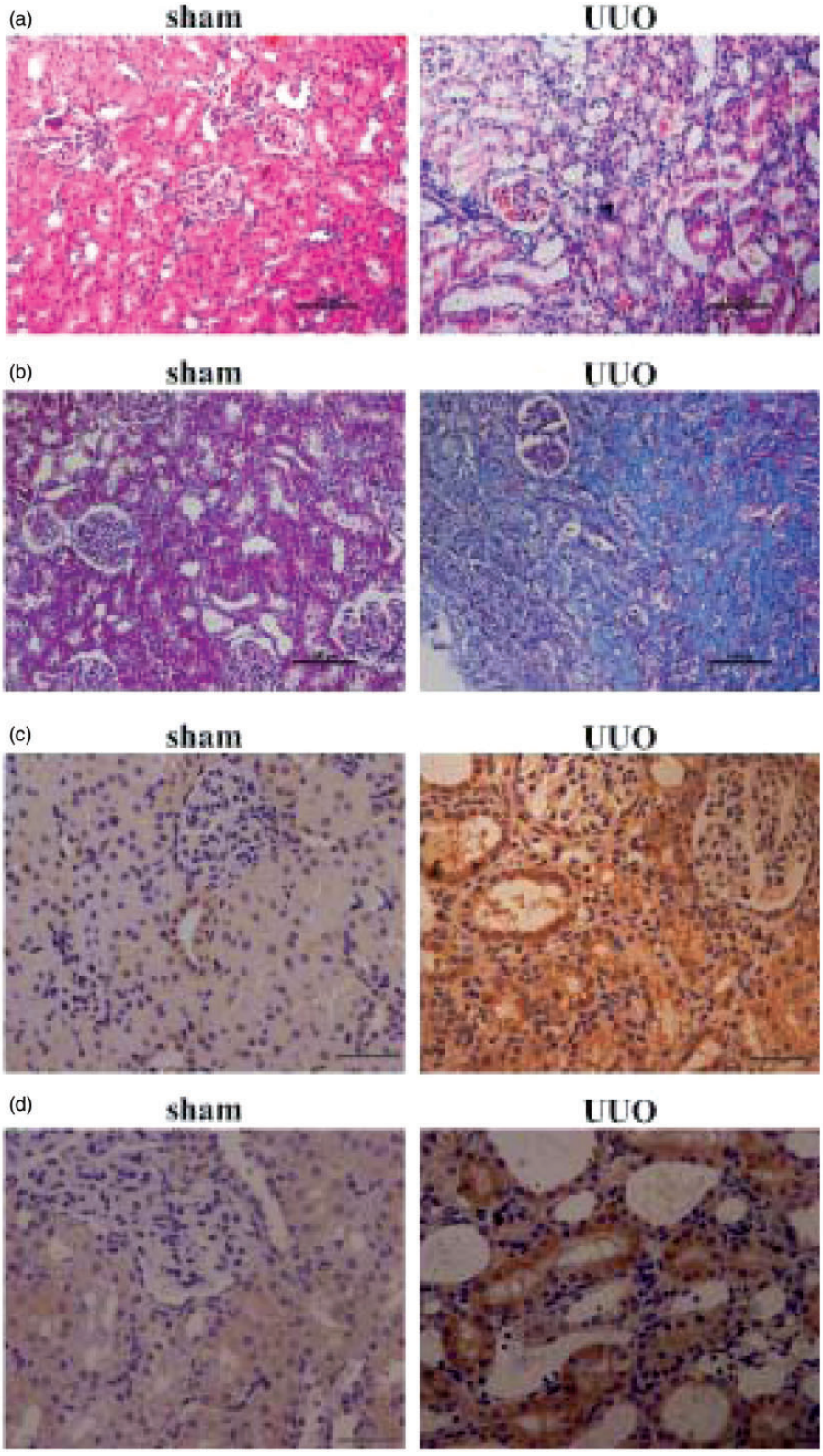

Figure 5 Location of BAG3 in kidneys from UUO rat model. (a) Representative images of HE staining in the kidney of rats on day 14 after the sham or UUO operation. The scale bar indicates 100 μm. (b) Representative images of Masson staining in the kidney of rats on day 14 after the sham or UUO operation. The scale bar indicates 100 μm. (c) Representative images of α-SMA staining in the kidney of rats on day 14 after the sham or UUO operation. The scale bar indicates 20 μm. (d) Representative images of BAG3 staining in the kidney of rats on day 14 after the sham or UUO operation. The scale bar indicates 20 μm. UUO: unilateral ureteral obstruction. (A color version of this figure is available in the online journal.)

might be helpful to clarify this issue in the future. In addition, more studies are necessary to clarify the detailed mechanisms underlying regulation of EMT by BAG3.

Taken together, the findings of the current study showed that FGF-2 induced the EMT of HK2 cells and coincided with the increase in BAG3 expression. Knockdown of BAG3 suppressed EMT, motion, and invasion of HK2 cells mediated by FGF-2. In addition, BAG3 was specifically increased in the tubular epithelium of UUO rats. These data highlight a substantial role of BAG3 in the EMT of renal tubular cells triggered by FGF-2, setting BAG3 as a potential target for the prevention and/or treatment of renal fibrosis.

Materials and methods

Cell culture

HK2 cells were cultured in Dulbecco's Minimum Essential Medium (DMEM)/F12 (Sigma–Aldrich, St. Louis, MO) supplemented with 10% fetal bovine serum (Sigma–Aldrich, St. Louis, MO).

RNA extraction and real-time reverse transcription (RT)-PCR

Total RNA was isolated from HK2 cells and real-time RT-PCR was performed as previously reported.[44] The following primer pairs were used: forward primer 5′-CATCCA GGAGTGCTGAAAGTG-3′ and reverse primer 5′-TCTGA ACCTTCCTGACACCG-3′ was used to detect BAG3 mRNA; forward primer 5′-GAGACCTTCAACACC CCAGCC-3′ and reverse primer 5′-GGATCTTCATGAG GTAGTCAG-3′ was used to measure β-actin mRNA. β-actin was used to normalize and results were presented as arbitrary unit.

Western blot analysis

Cellular protein was isolated from HK2 cells as previously reported.[29] Twenty-five micrograms of protein were separated with 12% sodium dodecyl sulfate polyacrylamide gel electropheresis (SDS-PAGE) and subsequently transferred to polyvinylidene fluoride (PVDF) membrane (Millipore Corporation, Billerica, MA). The following antibodies were used in the current study: a rabbit antibody against BAG3 (Abcam), a mouse antibody against α-SMA (Abcam), and a mouse antibody against glyceraldehyde 3-phosphate dehydrogenase (GAPDH) (Sigma–Aldrich).

Quantification of elongated cell morphology

F-actin was stained with rhodamine-labeled phalloidin and nuclei were counterstained with 4,6-diamino-2-phenylindole (DAPI). Images of cells were acquired using a 40× objective and the elongated cell morphology was determined as previously reported.[31] At least 50 cells for each experiment were measured.

Transduction of HK2 cells using lentiviral vectors

Lentiviral plasmids containing BAG3 shRNA and luciferase (LUC) shRNA target sequences and a GFP expression cassette were produced by GeneChem Corporation (Shanghai, China). The target sequences against BAG3 (shBAG3) were as follows: shBAG3#1 5′-AATTCAAGTGATCCGCAAA-3′; shBAG3#2 5′-ATCTCCATTCCGGTGATAC-3′; shBAG3#3 5′-AATTACCCATCACATAAAT-3′; and shBAG3#4 5′-TGGACACATCCCAATTCAA-3′. Target HK2 cells were incubated with vector supernatants for 12 h. Transduction efficiency was determined by the measurement of GFP+ cells by fluorescence microscopy. Transduced cells were cultured for two days before proteins were extracted and analyzed by western blot.

Scratch wound healing assay

Scratch wound healing experiments were performed as previously reported.[31] The experiments were performed three times independently. Multiple views of the leading edge of the scratch were photographed at 0 and 24 h from the scratching point, respectively.

Transwell invasion assays

Invasive capacity of cells was measured using *in vitro* Transwell invasion assays as previously reported.[31] Three experiments were performed independently. The cells passed through the filter were photographed and counted in five representative microscopic fields for each experiment.

Animals and the UUO model

All animal experiments were approved by Shengjing Hospital, China Medical University. The UUO animal model was generated in 8-week-old male Sprague–Dawley rats (weight 250–300 g). An intraperitoneal injection of ketamine (75 mg/kg body weight) was used to anesthetize the animals before a midline incision was performed to open the abdomen. Both proximal and distal points of the left ureter were ligated with 4.0 silk, and then the ureter was severed between these two ligation points to generate UUO. The abdominal cavity was then closed in layers. In the sham group, the left ureter was isolated but not ligated. Rats were killed at day 14 and after the operation.

Measurement of renal fibrosis

Paraffin sections (5 μm) of the kidney sections were stained with Masson's trichrome and scanned at 400× magnification by using NIS-Elements BR 2.10 image analysis software (Nikon, Tokyo, Japan).

Immunohistochemistry

Immunohistochemical staining was performed using the VECTASTAIN ABC systems according to the manufacturer's instructions (Vector Lab Inc). A mouse antibody against BAG3 (Enzo Life Sciences) and a mouse antibody against α-SMA (Abcam) was used to detect BAG3 and α-SMA, respectively. The sections were incubated with diaminobenzidine tetrahydrochloride in the presence of 3% hydrogen peroxide to visualize the antibodies.

RTCA proliferation assays

For RTCA proliferation experiments, cell proliferation was measured in a label-free real-time setting. Briefly, cells were seeded in RTCA E-plates (ACEA Bioscience, San Diego, CA) using xCELLigence RTCA DP (ACEA Bioscience, San Diego, CA). The proliferative rate of cells closely correlates with the increase in the electrical impedance on the plate, as an increase in the electrical impedance is observed when cells contact and adhere to the electronic sensors on the RTCA E-plate to proliferate.[45,46]

Trypan blue exclusion experiments

Cell viability was measured using trypan blue staining. After staining with trypan blue, viable (negative staining) and dead (positive staining) cell numbers were counted, respectively.

Statistics

All experiments were performed with triple repeats, and the mean ± standard deviation from a representative experiment was presented. Analysis of variance and post hoc Dunnett's test were used to determine the statistical significance of the difference and $P < .05$ was considered as statistical significance.

Authors' contributions: FD performed the molecular genetic studies, and participated in the study design and the data analysis. SL carried out infection, RTCA, and cell culture. TW carried out the cell count and wound-healing experiments. HYZ performed the cell culture and real-time PCR. DTL, ZXD, and HQW participated in study design, manuscript drafting, and data analysis. All authors proofread and approved the final manuscript.

ACKNOWLEDGEMENTS

This work was financially supported by National Natural Science Foundation of China (31170727, 31170745, and 81301838) and project supported by Scientific Research Fund of Liaoning Provincial Education Department (L2010581).

REFERENCES

1. Klionsky DJ, Abeliovich H, Agostinis P, Agrawal DK, Aliev G, Askew DS, *et al*. Guidelines for the use and interpretation of assays for monitoring autophagy in higher eukaryotes. *Autophagy* 2008;**4**:151–75
2. Hewitson TD. Renal tubulointerstitial fibrosis: common but never simple. *Am J Physiol Renal Physiol* 2009;**296**:F1239–44
3. Kalluri R, Neilson EG. Epithelial-mesenchymal transition and its implications for fibrosis. *J Clin Invest* 2003;**112**:1776–84
4. Nawrocki ST, Carew JS, Pino MS, Highshaw RA, Dunner K Jr., Huang P, Abbruzzese JL, McConkey DJ. Bortezomib sensitizes pancreatic cancer cells to endoplasmic reticulum stress-mediated apoptosis. *Cancer Res* 2005;**65**:11658–66
5. Liu Y. Cellular and molecular mechanisms of renal fibrosis. *Nat Rev Nephrol* 2011;**7**:684–96
6. Liu Y. New insights into epithelial-mesenchymal transition in kidney fibrosis. *J Am Soc Nephrol* 2010;**21**:212–22
7. Strutz FM. EMT and proteinuria as progression factors. *Kidney Int* 2009;**75**:475–81
8. Liu Y. Epithelial to mesenchymal transition in renal fibrogenesis: pathologic significance, molecular mechanism, and therapeutic intervention. *J Am Soc Nephrol* 2004;**15**:1–12
9. Thiery JP, Sleeman JP. Complex networks orchestrate epithelial-mesenchymal transitions. *Nat Rev Mol Cell Biol* 2006;**7**:131–42
10. Savagner P. Leaving the neighborhood: molecular mechanisms involved during epithelial-mesenchymal transition. *Bioessays* 2001;**23**:912–23
11. Voulgari A, Pintzas A. Epithelial-mesenchymal transition in cancer metastasis: mechanisms, markers and strategies to overcome drug resistance in the clinic. *Biochim Biophys Acta* 2009;**1796**:75–90
12. Masola V, Gambaro G, Tibaldi E, Brunati AM, Gastaldello A, D'Angelo A, Onisto M, Lupo A. Heparanase and syndecan-1 interplay orchestrates fibroblast growth factor-2-induced epithelial-mesenchymal transition in renal tubular cells. *J Biol Chem* 2012;**287**:1478–88
13. Strutz F, Zeisberg M, Ziyadeh FN, Yang CQ, Kalluri R, Muller GA, Neilson EG. Role of basic fibroblast growth factor-2 in epithelial-mesenchymal transformation. *Kidney Int* 2002;**61**:1714–28
14. Antoku K, Maser RS, Scully WJ Jr., Delach SM, Johnson DE. Isolation of Bcl-2 binding proteins that exhibit homology with BAG-1 and suppressor of death domains protein. *Biochem Biophys Res Commun* 2001;**286**:1003–10
15. Doong H, Price J, Kim YS, Gasbarre C, Probst J, Liotta LA, Blanchette J, Rizzo K, Kohn E. CAIR-1/BAG-3 forms an EGF-regulated ternary complex with phospholipase C-gamma and Hsp70/Hsc70. *Oncogene* 2000;**19**:4385–95
16. Homma S, Iwasaki M, Shelton GD, Engvall E, Reed JC, Takayama S. BAG3 deficiency results in fulminant myopathy and early lethality. *Am J Pathol* 2006;**169**:761–73
17. Hishiya A, Kitazawa T, Takayama S. BAG3 and Hsc70 interact with actin capping protein CapZ to maintain myofibrillar integrity under mechanical stress. *Circ Res* 2010;**107**:1220–31
18. Pagliuca MG, Lerose R, Cigliano S, Leone A. Regulation by heavy metals and temperature of the human BAG-3 gene, a modulator of Hsp70 activity. *FEBS Lett* 2003;**541**:11–15
19. Bonelli P, Petrella A, Rosati A, Romano MF, Lerose R, Pagliuca MG, Amelio T, Festa M, Martire G, Venuta S, Turco MC, Leone A. BAG3 protein regulates stress-induced apoptosis in normal and neoplastic leukocytes. *Leukemia* 2004;**18**:358–60
20. Chen L, Wu W, Dentchev T, Zeng Y, Wang J, Tobias JW, Bennett J, Baldwin D, Dunaief JL. Light damage induced changes in mouse retinal gene expression. *Exp Eye Res* 2004;**79**:239–47
21. Tabuchi Y, Ando H, Takasaki I, Feril LB Jr., Zhao QL, Ogawa R, Kudo N, Tachibana K, Kondo T. Identification of genes responsive to low intensity pulsed ultrasound in a human leukemia cell line Molt-4. *Cancer Lett* 2007;**246**:149–56
22. Wang HQ, Liu HM, Zhang HY, Guan Y, Du ZX. Transcriptional upregulation of BAG3 upon proteasome inhibition. *Biochem Biophys Res Commun* 2008;**365**:381–85
23. Du ZX, Zhang HY, Meng X, Gao YY, Zou RL, Liu BQ, Guan Y, Wang HQ. Proteasome inhibitor MG132 induces BAG3 expression through activation of heat shock factor 1. *J Cell Physiol* 2009;**218**:631–37
24. Iwasaki M, Homma S, Hishiya A, Dolezal SJ, Reed JC, Takayama S. BAG3 regulates motility and adhesion of epithelial cancer cells. *Cancer Res* 2007;**67**:10252–59
25. Suzuki M, Iwasaki M, Sugio A, Hishiya A, Tanaka R, Endo T, Takayama S, Saito T. BAG3 (BCL2-associated athanogene 3) interacts with MMP-2 to positively regulate invasion by ovarian carcinoma cells. *Cancer Lett* 2011;**303**:65–71
26. Kassis JN, Guancial EA, Doong H, Virador V, Kohn EC. CAIR-1/BAG-3 modulates cell adhesion and migration by downregulating activity of focal adhesion proteins. *Exp Cell Res* 2006;**312**:2962–71
27. McCollum AK, Casagrande G, Kohn EC. Caught in the middle: the role of Bag3 in disease. *Biochem J* 2010;**425**:e1–3
28. Liu BQ, Du ZX, Zong ZH, Li C, Li N, Zhang Q, Kong DH, Wang HQ. BAG3-dependent noncanonical autophagy induced by proteasome inhibition in HepG2 cells. *Autophagy* 2013;**9**:905–16

29. Li C, Li S, Kong DH, Meng X, Zong ZH, Liu BQ, Guan Y, Du ZX, Wang HQ. BAG3 is upregulated by c-Jun and stabilizes JunD. *Biochim Biophys Acta* 2013;**1833**:3346–54
30. Kong DH, Zhang Q, Meng X, Zong ZH, Li C, Liu BQ, Guan Y, Wang HQ. BAG3 sensitizes cancer cells exposed to DNA damaging agents via direct interaction with GRP78. *Biochim Biophys Acta* 2013;**1833**:3245–53
31. Li N, Du ZX, Zong ZH, Liu BQ, Li C, Zhang Q, Wang HQ. PKC delta-mediated phosphorylation of BAG3 at Ser187 site induces epithelial--mesenchymal transition and enhances invasiveness in thyroid cancer FRO cells. *Oncogene* 2013;**32**:4539–48
32. Gentilella A, Khalili K. BAG3 expression is sustained by FGF2 in neural progenitor cells and impacts cell proliferation. *Cell Cycle* 2010;**9**:4245–47
33. Gentilella A, Passiatore G, Deshmane S, Turco MC, Khalili K. Activation of BAG3 by Egr-1 in response to FGF-2 in neuroblastoma cells. *Oncogene* 2008;**27**:5011–8
34. Kaneto H, Morrissey J, McCracken R, Reyes A, Klahr S. Enalapril reduces collagen type IV synthesis and expansion of the interstitium in the obstructed rat kidney. *Kidney Int* 1994;**45**:1637–47
35. Picard N, Baum O, Vogetseder A, Kaissling B, Le Hir M. Origin of renal myofibroblasts in the model of unilateral ureter obstruction in the rat. *Histochem Cell Biol* 2008;**130**:141–55
36. Lee JH, Takahashi T, Yasuhara N, Inazawa J, Kamada S, Tsujimoto Y. Bis, a Bcl-2-binding protein that synergizes with Bcl-2 in preventing cell death. *Oncogene* 1999;**18**:6183–90
37. Takayama S, Xie Z, Reed JC. An evolutionarily conserved family of Hsp70/Hsc70 molecular chaperone regulators. *J Biol Chem* 1999;**274**:781–86
38. Chevalier RL, Forbes MS, Thornhill BA. Ureteral obstruction as a model of renal interstitial fibrosis and obstructive nephropathy. *Kidney Int* 2009;**75**:1145–52
39. Bani-Hani AH, Campbell MT, Meldrum DR, Meldrum KK. Cytokines in epithelial-mesenchymal transition: a new insight into obstructive nephropathy. *J Urol* 2008;**180**:461–68
40. Skaletz-Rorowski A, Eschert H, Leng J, Stallmeyer B, Sindermann JR, Pulawski E, Breithardt G. PKC delta-induced activation of MAPK pathway is required for bFGF-stimulated proliferation of coronary smooth muscle cells. *Cardiovasc Res* 2005;**67**:142–50
41. Wang J, Nachtigal MW, Kardami E, Cattini PA. FGF-2 protects cardiomyocytes from doxorubicin damage via protein kinase C-dependent effects on efflux transporters. *Cardiovasc Res* 2013;**98**:56–63
42. Yang QE, Johnson SE, Ealy AD. Protein kinase C delta mediates fibroblast growth factor-2-induced interferon-tau expression in bovine trophoblast. *Biol Reprod* 2011;**84**:933–43
43. Jiang CC, Mao ZG, Avery-Kiejda KA, Wade M, Hersey P, Zhang XD. Glucose-regulated protein 78 antagonizes cisplatin and adriamycin in human melanoma cells. *Carcinogenesis* 2009;**30**:197–204
44. Wang HQ, Du ZX, Zhang HY, Gao DX. Different induction of GRP78 and CHOP as a predictor of sensitivity to proteasome inhibitors in thyroid cancer cells. *Endocrinology* 2007;**148**:3258–70
45. Solly K, Wang X, Xu X, Strulovici B, Zheng W. Application of real-time cell electronic sensing (RT-CES) technology to cell-based assays. *Assay Drug Dev Technol* 2004;**2**:363–72
46. Ke N, Wang X, Xu X, Abassi YA. The xCELLigence system for real-time and label-free monitoring of cell viability. *Methods Mol Biol* 2011;**740**:33–43

(Received May 24, 2014, Accepted September 11, 2014)